Gang-Feng Wang[1]
MOE Key Laboratory for Strength and Vibration,
Department of Engineering Mechanics,
Xi'an Jiaotong University,
Xi'an 710049, China
e-mail: wanggangfeng@tsinghua.org.cn

Xi-Qiao Feng
Department of Engineering Mechanics,
Tsinghua University,
Beijing 100084, China

Tie-Jun Wang
MOE Key Laboratory for Strength and Vibration,
Department of Engineering Mechanics,
Xi'an Jiaotong University,
Xi'an 710049, China

Wei Gao
Department of Engineering Mechanics,
Tsinghua University,
Beijing 100084, China

Surface Effects on the Near-Tip Stresses for Mode-I and Mode-III Cracks

Based on the surface elasticity theory and using a local asymptotic approach, we analyzed the influences of surface energy on the stress distributions near a blunt crack tip. The dependence relationship of the crack-tip stresses on surface elastic parameters is obtained for both mode-I and mode-III cracks. It is found that when the curvature radius of a crack front decreases to nanometers, surface energy significantly affects the stress intensities near the crack tip. Using a kind of surface elements, we also performed finite element simulations to examine the surface effects on the near-tip stresses. The obtained analytical solution agrees well with the numerical results. [DOI: 10.1115/1.2712233]

Keywords: crack, surface elasticity, stress, nanomechanics

1 Introduction

Analysis of deformations and stresses at crack tips is a fundamental issue for understanding the failure behavior of engineering materials and structures. At macroscopic scale, the crack front profile is usually considered to be infinitely sharp, and the corresponding elastic and elastic-plastic crack-tip fields have been well established in the classical fracture mechanics. In physical nature, however, most crack tips are not ideally sharp but blunt with a finite curvature radius, e.g., on the order of microns or nanometers. First, only when the spacing between the two surfaces of a crack is larger enough beyond some physical limits (e.g., the cutoff radius of Lennard-Jones potential), are the surfaces free from atomic interaction. Second, the atoms near a crack tip experience a local environment different from those in the bulk, and their tendency to minimize the system free energy may also cause blunting of the crack tip.

Atomic simulation is very powerful in pursuing the details of deformations and evolution processes at nanoscale, and has been employed to investigate fracture problems [1–4]. Through massively parallel atomistic simulations, Buehler and Gao [1] and Buehler et al. [2] reported the dynamical fracture instabilities due to local hyperelasticity at crack tips. Abraham et al. [4] developed a concurrent multiscale method spanning the continuum to quantum length scales to study brittle fracture problems.

Recently, continuum mechanics models of surface elasticity have also been adopted to explore the features of mechanical deformations at nanoscale by incorporating the effects of surface/interface energy [5–9]. The generic and mathematical formulation of surface elasticity theory was presented by Gurtin and Murdoch [10] and Gurtin et al. [11], in which a surface is regarded as a two-dimensional membrane adhered to the bulk without slipping. Experiments on some elementary deformation modes, such as uniaxial stretching of plates, bending of beams, and torsion of bars, showed that the predictions from the surface elasticity theory agrees well with the results from directly atomic simulations [5,6]. Therefore, the surface elasticity theory has been employed to elucidate many size-dependent phenomena at nanoscale, for examples, the deformation around a spherical nanoinhomogeneity [7], the effective modulus of elastic solid with nanocavities [12,13] and nanoinclusions [14,15]. In addition, based on the analysis for an elliptic void, Wu [16] addressed the effect of surface stress on the deformation of a crack, in which only the constant residual surface stress is considered.

Through the embedded atom method, Hoagland et al. [17] examined the deformation field near a crack tip. They found that the stresses calculated from atomic models are in a good agreement with the predictions of linear elastic fracture mechanics except in a small vicinity of the crack tip, where the effects of surface energy should be accounted for. Therefore, local analysis near a crack tip may capture the key features of surface effects on crack tip fields. Creager and Paris [18] and Smith [19] investigated the stress distributions near the tip of a blunt crack in the light of classical elastic theory. In the present paper, we will use Gurtin's surface elasticity theory to examine the surface effects on the deformations and stresses in the immediate vicinity of a blunt crack tip.

The paper is organized as follows. The basic equations of Gurtin's surface elasticity theory are reviewed briefly in Sec. 2. In Secs. 3 and 4, the stress distributions near the tips of mode-III and mode-I cracks are determined through a local approach. In Sec. 5, the obtained theoretical results are compared to our finite element simulations with surface effects.

2 Basic Equations of Surface Elasticity

In Gurtin's surface elasticity theory [11], a surface is regarded as an elastic but negligibly thin membrane, which is adhered to the underlying bulk material without slipping and has elastic constants different from the bulk. The surface stress tensor is a function of the surface strain tensor, which depends on the deformation of the bulk material. The equilibrium and constitutive equations in the bulk of the material are the same as those in the classical theory of elasticity, but the presence of surface stress gives rise to a nonclassical boundary condition. Only several basic equations of the surface elasticity theory are reviewed here. For its detailed mathematical formulation, the reader may refer to Gurtin and Murdoch [10] and Gurtin et al. [11].

[1]Corresponding author.

Contributed by the Applied Mechanics Division of ASME for publication in the JOURNAL OF APPLIED MECHANICS. Manuscript received May 10, 2006; final manuscript received October 23, 2006; published online December 27, 2007. Review conducted by Zhigang Suo.

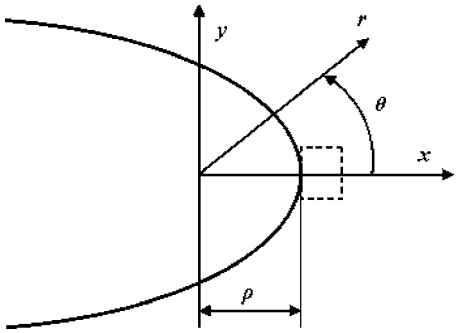

Fig. 1 A blunt crack with a finite curvature radius at its tip

In the absence of body forces, the equilibrium equations and the isotropic constitutive relations in the bulk read

$$\sigma_{ij,j} = 0 \tag{1}$$

$$\sigma_{ij} = 2G\varepsilon_{ij} + \lambda\varepsilon_{kk}\delta_{ij} \tag{2}$$

where G and λ are the Lame constants, σ_{ij} and ε_{ij} are the stress tensor and strain tensor in the bulk material, respectively. The strain tensor is related to the displacement vector u_i by

$$\varepsilon_{ij} = \tfrac{1}{2}(u_{i,j} + u_{j,i}) \tag{3}$$

Throughout the paper, Einstein's summation convention is adopted for all repeated Latin indices (1, 2, 3) and Greek indices (1, 2).

Assume that the surface adheres perfectly to the bulk material without slipping. The equilibrium conditions on the surface are obtained as

$$t_\alpha + \sigma^s_{\beta\alpha,\beta} = 0, \quad \sigma_{ij}n_i n_j = \sigma^s_{\alpha\beta}\kappa_{\alpha\beta} \tag{4}$$

where n_i denotes the outward normal vector to the surface, t_α is the negative of the tangential component of the traction $t_i = \sigma_{ij}n_j$ along the α_i direction of surface, $\kappa_{\alpha\beta}$ is the surface curvature tensor.

The surface stress tensor $\sigma^s_{\alpha\beta}$ is related to the surface energy density $\Gamma(\varepsilon_{\alpha\beta})$ by

$$\sigma^s_{\alpha\beta} = \tau^0\delta_{\alpha\beta} + \frac{\partial\Gamma}{\partial\varepsilon_{\alpha\beta}} \tag{5}$$

where $\delta_{\alpha\beta}$ is the Kronecker δ, $\varepsilon_{\alpha\beta}$ the second-rank tensor of surface strains, and τ^0 the residual surface tension under unstrained condition. For an isotropic surface, the surface stresses are given by

$$\sigma^s_{\alpha\beta} = \tau^0\delta_{\alpha\beta} + 2(\mu^s - \tau^0)\delta_{\alpha\gamma}\varepsilon_{\gamma\beta} + (\lambda^s + \tau^0)\varepsilon_{\gamma\gamma}\delta_{\alpha\beta} \tag{6}$$

where μ^s and λ^s are surface elastic constants.

3 Near-Tip Deformation for Mode-III Crack

Now we consider the deformation near a two-dimensional crack tip, which has an initially blunt shape of curvature radius ρ. Refer to a Cartesian coordinate system (x,y) and a polar coordinate system (r,θ), as shown in Fig. 1. The origin of the coordinate systems is located at the curvature center of the crack tip, and the z-axis is normal to the x-y plane.

For mode-III problems, the only nonvanishing displacement w along z-axis satisfies the Laplace's equation

$$\frac{\partial^2 w}{\partial x^2} + \frac{\partial^2 w}{\partial y^2} = 0 \tag{7}$$

The displacement w can be given by an analytical function $F(z)$ of $z = x + y\mathrm{i}$ as

$$Gw = \mathrm{Re}[F(z)] \tag{8}$$

and the stress components are expressed as

$$\sigma_{r3} - \mathrm{i}\sigma_{\theta 3} = \exp(\mathrm{i}\theta)\frac{\mathrm{d}F}{\mathrm{d}z} \tag{9}$$

As it has been found from atomic simulations [17], the influence of surface energy is localized near the crack tip. Therefore, we use a local analysis to focus on an immediate vicinity of the crack tip for $|z-\rho| \ll \rho$. Hereby, $F(z)$ can be expressed in power series of $(z-\rho)$ as

$$F(z) = a_0 + \mathrm{i}b_0 + (a_1 + \mathrm{i}b_1)(z-\rho) + (a_2 + \mathrm{i}b_2)(z-\rho)^2 + o\{(z-\rho)^2\} \tag{10}$$

where a_0, b_0, a_1, b_1, a_2, and b_2 are real constants. Then to the first order of $(z-\rho)$, the stresses are given from Eqs. (9) and (10) as

$$\begin{aligned}\sigma_{r3} &= a_1\cos\theta - b_1\sin\theta + 2r(a_2\cos 2\theta - b_2\sin 2\theta) - 2\rho(a_2\cos\theta \\ &\quad - b_2\sin\theta) \\ \sigma_{\theta 3} &= -(b_1\cos\theta + a_1\sin\theta) - 2r(b_2\cos 2\theta + a_2\sin 2\theta) \\ &\quad + 2\rho(b_2\cos\theta + a_2\sin\theta)\end{aligned} \tag{11}$$

The corresponding nonvanishing strain components are

$$\varepsilon_{r3} = \varepsilon_{3r} = \frac{\sigma_{r3}}{2G}, \quad \varepsilon_{\theta 3} = \varepsilon_{3\theta} = \frac{\sigma_{\theta 3}}{2G} \tag{12}$$

Then one obtains the surface stress components on the crack surface

$$\sigma^s_{3\theta} = \sigma^s_{\theta 3} = 2G^s\varepsilon_{3\theta}, \quad \sigma^s_{33} = \sigma^s_{\theta\theta} = \tau^0 \tag{13}$$

with $G^s = \mu^s - \tau^0$.

On the crack surface near the tip $(r=\rho)$, the surface boundary condition in Eq. (4) reduces to

$$\sigma_{r3} = -\frac{\partial\sigma^s_{\theta 3}}{r\partial\theta} \tag{14}$$

Substitution of Eqs. (11)–(13) into Eq. (14) leads to

$$\begin{aligned}&a_1\cos\theta - b_1\sin\theta + 2\rho(a_2\cos 2\theta - b_2\sin 2\theta) - 2\rho(a_2\cos\theta \\ &\quad - b_2\sin\theta) \\ &= -\frac{G^s}{G\rho}[b_1\sin\theta - a_1\cos\theta + 4\rho(b_2\sin 2\theta - a_2\cos 2\theta) \\ &\quad + 2\rho(a_2\cos\theta - b_2\sin\theta)]\end{aligned} \tag{15}$$

For a small value of θ near the crack tip, we expand Eq. (15) in terms of θ up to the square order; that is,

$$\begin{aligned}&a_1 - \theta(b_1 + 2\rho b_2) - \theta^2\left(\frac{a_1}{2} + 3\rho a_2\right) \\ &\quad = \frac{G^s}{G\rho}\left[2\rho a_2 + a_1 - \theta(b_1 + 6\rho b_2) - \theta^2\left(\frac{a_1}{2} + 7\rho a_2\right)\right]\end{aligned} \tag{16}$$

Comparing the factors of 1, θ and θ^2 at the two sides of Eq. (16) gives

$$a_1 = a_2 = 0, \quad b_2 = -\frac{b_1}{2\rho}\left(\frac{\rho G - G^s}{\rho G - 3G^s}\right) \tag{17}$$

Then the shear stress at the crack tip $(r=\rho,\ \theta=0)$ is obtained as

$$\sigma^p_{\theta 3} = \sigma_{\theta 3}(\rho, 0) = -b_1 \tag{18}$$

If no effect of surface elasticity is considered, Eq. (18) should reduce to the solution of classical linear elasticity. Therefore, the parameter b_1 can be determined from the linear elastic fracture mechanics. Since the surface constants do not appear in Eq. (18), surface energy does not affect the stresses at the tip of a mode-III crack.

However, at a distance t ahead of the crack tip ($r=\rho+t$, $\theta=0$), the shear stress is given by

$$\frac{\sigma_{\theta 3}}{\sigma_{\theta 3}^{p}} = 1 - \frac{t}{\rho}k \tag{19}$$

with $k=(\rho G-G^s)/(\rho G-3G^s)$.

Equation (19) clearly demonstrates that the stress depends not only on t, ρ, and $\sigma_{\theta 3}^{p}$ but also on the surface constant G^s. Its last term stands for the relative influence of surface elasticity on the stress. For metals, G^s/G is usually on the order of nanometers [5,7,12]. Therefore, it is only when the curvature radius ρ is of the order of nanometers that the effects of surface energy become significant. For a very blunt crack ($\rho \gg G^s/G$), $k \to 1$ and the result reduces to that of classical elasticity analysis [19]. For a very sharp crack ($\rho \ll G^s/G$ and $k \to 1/3$), however, the solution in Eq. (19) is different distinctly from that of classical elasticity.

4 Near-Tip Deformation for Mode-I Crack

Then we consider the deformation near the tip of a mode-I crack under plane-strain conditions. In this case, $\varepsilon_{\theta\theta}$ is the only nonzero surface strain on the crack surface, and the surface stress $\sigma_{\theta\theta}^{s}$ is given by

$$\sigma_{\theta\theta}^{s} = \tau^0 + E^s \varepsilon_{\theta\theta} \tag{20}$$

with $E^s=2\mu^s+\lambda^s-\tau^0$ being the surface elastic modulus.

On the crack surface near the tip, the surface boundary conditions in Eq. (4) are simplified as

$$\sigma_{rr} = \frac{\sigma_{\theta\theta}^{(s)}}{\rho}, \quad \sigma_{r\theta} = -\frac{\partial \sigma_{\theta\theta}^{(s)}}{\rho \partial \theta} \tag{21}$$

According to the complex variable formulation [20], the stresses in the bulk can be expressed by two analytic functions $\phi(z)$ and $\psi(z)$ of $z=x+iy$ as

$$\sigma_{rr}+\sigma_{\theta\theta} = 2[\phi(z)+\overline{\phi(z)}],$$

$$\sigma_{\theta\theta}-\sigma_{rr}+2i\sigma_{r\theta} = 2[\bar{z}\phi'(z)+\psi(z)]\exp(2i\theta) \tag{22}$$

Because of the special significance of the stress values at the crack tip for the initiation of fracture, we are concerned mainly with the surface elasticity effects on the stress strength in the immediate vicinity of the crack tip ($|z-\rho| \ll \rho$). The analytic functions $\phi(z)$ and $\psi(z)$ can be expressed in the form of power series as

$$\phi(z) = (a_0+ib_0)+(a_1+ib_1)(z-\rho)+(a_2+ib_2)(z-\rho)^2+o\{(z-\rho)^2\}$$

$$\psi(z) = (c_0+id_0)+(c_1+id_1)(z-\rho)+o\{(z-\rho)\} \tag{23}$$

where a_0, b_0, a_1, b_1, a_2, b_2, c_0, d_0, c_1, and d_1 are all real constants. Substituting Eq. (23) into (22) leads to the following expressions of stress components to the first order of $(z-\rho)$:

$$\sigma_{rr}+\sigma_{\theta\theta} = 2[2a_0+(a_1+ib_1)(z-\rho)+(a_1-ib_1)(\bar{z}-\rho)]$$

$$\sigma_{\theta\theta}-\sigma_{rr}+2i\sigma_{r\theta} = 2\exp(2i\theta)\{\bar{z}[a_1+ib_1+2(a_2+ib_2)(z-\rho)]+c_0+id_0+(c_1+id_1)(z-\rho)\} \tag{24}$$

On the crack surface $z=\rho\exp(i\theta)$, the stress components are expressed as

$$\sigma_{rr} = 2a_0-2\rho a_1+\rho a_1\cos\theta-\rho b_1\sin\theta-c_0\cos 2\theta+d_0\sin 2\theta-2\rho^2 a_2(\cos 2\theta-\cos\theta)+2\rho^2 b_2(\sin 2\theta-\sin\theta)-\rho c_1(\cos 3\theta-\cos 2\theta)+\rho d_1(\sin 3\theta-\sin 2\theta)$$

$$\sigma_{r\theta} = \rho a_1\sin\theta+\rho b_1\cos\theta+d_0\cos 2\theta+c_0\sin 2\theta+2\rho^2 a_2(\sin 2\theta-\sin\theta)+2\rho^2 b_2(\cos 2\theta-\cos\theta)+\rho d_1(\cos 3\theta-\cos 2\theta)+\rho c_1(\sin 3\theta-\sin 2\theta)$$

$$\sigma_{\theta\theta} = 2a_0+(3\cos\theta-2)\rho a_1-3\rho b_1\sin\theta+c_0\cos 2\theta-d_0\sin 2\theta+2\rho^2 a_2(\cos 2\theta-\cos\theta)-2\rho^2 b_2(\sin 2\theta-\sin\theta)+\rho c_1(\cos 3\theta-\cos 2\theta)-\rho d_1(\sin 3\theta-\sin 2\theta)$$

$$\sigma_{zz} = \nu(\sigma_{rr}+\sigma_{\theta\theta}) \tag{25}$$

For the considered plane-strain problem, the strain $\varepsilon_{\theta\theta}$ is given by

$$\varepsilon_{\theta\theta} = \frac{1}{2G}[(1-\nu)\sigma_{\theta\theta}-\nu\sigma_{rr}] \tag{26}$$

where ν is the Poisson's ratio.

From Eqs. (25), (26), and (20), one can obtain the surface stress $\sigma_{\theta\theta}^{s}$ on the crack surface. Analogously to the derivation in Sec. 3, we substitute the stresses and surface stress into the boundary conditions in Eq. (21), expand the relations in terms of θ up to the square order and compare the coefficients of 1, θ, and θ^2. Then the constants a_1, b_1, a_2, b_2, c_1, and d_1 are obtained in terms of a_0, b_0, c_0, and d_0 as

$$a_1 = \frac{2a_0-c_0-\tau^0/\rho-2a_0\eta+4\eta\nu a_0-\eta c_0}{(\eta+1)\rho}$$

$$b_1 = \frac{1+\eta}{3\eta-4\nu\eta-1}\left(\frac{d_0}{\rho}\right)$$

$$c_1 = \{4a_0-c_0+(32\nu^2 a_0-8\nu c_0+7c_0+12a_0-40\nu a_0)\eta^2+(6c_0-8\nu c_0-16a_0+24\nu a_0)\eta+(6\eta-8\eta\nu-2)\tau^0/\rho\}/\{(1+\eta)^2\rho\}$$

$$d_1 = \left(\frac{1-2\eta}{1-6\eta}\right)\left(\frac{3d_0}{\rho}\right)$$

$$a_2 = 3\{-2a_0+(1+4\eta\nu-3\eta)\tau^0/\rho-12\eta\nu a_0-4\eta c_0+8\eta a_0-6a_0+4\eta\nu c_0+(20\nu a_0-16\nu^2 a_0+4\nu c_0-4c_0-6a_0)\eta^2\}/\{2(1+\eta)^2\rho^2\}$$

$$b_2 = \left(\frac{4\eta-1}{1-6\eta}\right)\left(\frac{3d_0}{\rho^2}\right) \tag{27}$$

where the nondimensional parameter $\eta=E^s/(2G\rho)$ signifies the surface effects.

Then the stresses at the crack tip ($r=\rho$, $\theta=0$) are determined as

$$\sigma_{yy}^{p} = \sigma_{yy}^{0}\left(\frac{1+\eta\nu}{1+\eta}\right)-\frac{\tau^0}{(1+\eta)\rho}$$

$$\sigma_{xy}^{p} = \frac{4d_0\eta(\nu-1)}{1-3\eta+4\eta\nu}$$

$$\sigma_{xx}^{p} = \sigma_{yy}^{0}\frac{\eta(1-\nu)}{1+\eta}+\frac{\tau^0}{(1+\eta)\rho} \tag{28}$$

where $\sigma_{yy}^{0}=4a_0$ stands for the stress $\sigma_{yy}(\rho,0)$ at the crack tip without surface effects. It is seen from Eq. (28) that the surface energy significantly alters the near-tip stresses, which rely on the surface constants and the curvature radius of the crack tip.

Equation (28) should reduce to the solution of classical linear elastic fracture mechanics if the effect of surface elasticity is neglected (i.e., $\eta=0$ and $\tau^0=0$). Therefore, the parameters a_0 and d_0 can be determined from the well-known K-field solution of linear elasticity. From the solution for a blunt mode-I crack [18], it is obtained $\sigma_{yy}^{0}=4a_0=2K_I/\sqrt{\pi\rho}$ and $d_0=0$, where K_I is the stress intensity factor in the far field.

For $\eta=0$ and $\tau^0 \neq 0$, Eq. (28) reduces to $\sigma_{yy}^{p}/\sigma_{yy}^{0}=1-\tau^0/(\sigma_{yy}^{0}\rho)$. The contribution from surface energy is completely determined by the residual surface stress and the root radius. For a very blunt crack ($\rho \gg \tau^0/\sigma_{yy}^{0}$), $\sigma_{yy}^{p}/\sigma_{yy}^{0} \to 1$ and then the influ-

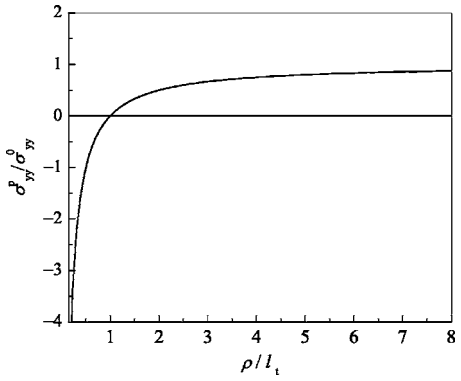

Fig. 2 Variation of $\sigma_{yy}^p/\sigma_{yy}^0$ with respect to the curvature radius for $\eta=0$

ence of surface energy is negligible. But for a very sharp crack ($\rho \sim \tau^0/\sigma_{yy}^0$), the contribution from surface energy should be taken into account. For a mode-I crack, the variation of $\sigma_{yy}^p/\sigma_{yy}^0$ with respect to the curvature radius of the crack tip is shown in Fig. 2, where $l_t=\tau^0/\sigma_{yy}^0$. The curvature radius not only affects the magnitude of stress, but changes its deformation state from stretching to compression. A positive residual surface stress in front of a mode-I crack may postpone its propagation and therefore enhances the fracture toughness of the material. But a negative residual surface stress will lower the fracture toughness of the material. These conclusions are in qualitative agreement with those in Wu [16], where the stress intensity factor is analyzed using the assumption of constant surface stress.

For $\tau^0=0$ and $\eta \neq 0$, Eq. (28) simplifies to $\sigma_{yy}^p/\sigma_{yy}^0=(1+\eta\nu)/(1+\eta)$. For metals, $l_s=E^s/(2G)$ is usually on the order of nanometers [5,7,12]. Therefore, it is seen from Eq. (28) and $\eta=l_s/\rho$ that only when the curvature radius at the crack tip reduces to nanometers do the surface effects become significant. For a very blunt crack ($\rho \gg l_s$), $\eta \to 0$ and $\sigma_{yy}^p/\sigma_{yy}^0 \to 1$, whereas for a very sharp crack ($\rho \ll l_s$), $\eta \to \infty$ and $\sigma_{yy}^p/\sigma_{yy}^0 \to \nu$. With the decrease in the crack root curvature radius, the stress ratio $\sigma_{yy}^p/\sigma_{yy}^0$ reduces continuously from 1 to ν, as shown in Fig. 3.

5 Finite Element Formulation of Surface Elasticity

To examine the accuracy of the analytical solution in Eq. (28), we also carried out finite element simulations to calculate the stress distributions near the crack tip. The surface element developed recently by Gao et al. [13] is used to account for the effects of surface elasticity.

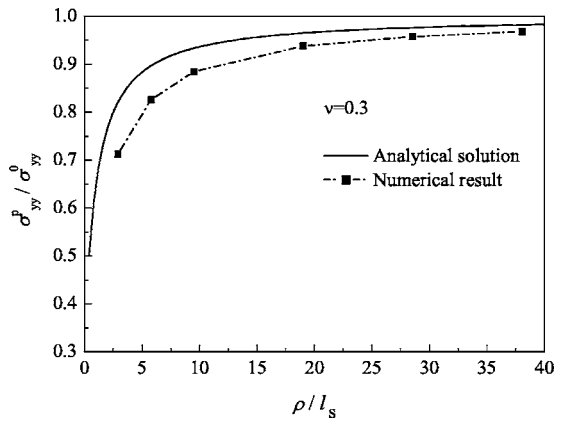

Fig. 3 Variation of $\sigma_{yy}^p/\sigma_{yy}^0$ with respect to the curvature radius for $\tau^0=0$

The total potential energy Π in the surface elasticity theory consists of three parts, the bulk elastic energy U^b, the surface elastic energy U^s, and the work of external force W, i.e.,

$$\prod = U^b + U^s - W \tag{29}$$

U^b and W can be calculated from the bulk elements as in the classical elasticity.

For elements on surfaces or interfaces, we incorporate the influence of surface energy. The surface energy for each surface element is given by [13]

$$U^s = \int_\Omega \int \{\sigma^s\}^T d\{\varepsilon^s\} d\Omega \tag{30}$$

where Ω is the area of surface element, $\{\sigma^s\}$ and $\{\varepsilon^s\}$ are the surface stress matrix and the surface strain matrix, respectively. Substituting Eq. (5) into Eq. (30), the surface energy is rewritten as

$$U^s = \frac{1}{2}\int_\Omega \{\varepsilon^s\}^T[S]\{\varepsilon^s\} d\Omega + \int_\Omega \{\varepsilon^s\}^T\{F\} d\Omega \tag{31}$$

where $[S]$ and $[F]$ stand for the surface elastic matrix and residual surface stress matrix, respectively. For a surface adhered perfectly to the bulk, the surface strains of a surface element can be determined by its adjacent bulk element via the relation

$$\{\varepsilon^s\} = [B^s]\{\delta_e\} \tag{32}$$

where $[B^s]$ is the strain-displacement matrix of the surface element, and $\{\delta_e\}$ the nodal displacement matrix of bulk element. Therefore, the surface energy can be expressed as

$$U^s = \tfrac{1}{2}\{\delta_e\}^T[K_e^s]\{\delta_e\} + \{\delta_e\}^T\{P_e^s\} \tag{33}$$

where $[K_e^s]$ and $\{P_e^s\}$ are the surface stiffness matrix and the surface residual stress matrix, respectively. They are defined as

$$[K_e^s] = \int_\Omega \{B^s\}^T[S]\{B^s\} d\Omega \tag{34}$$

$$\{P_e^s\} = \int_\Omega \{B^s\}^T\{F\} d\Omega \tag{35}$$

According to the principle of minimum potential energy, the relationships between the nodal displacements and the nodal forces read

$$\{[K_e] + [K_e^s]\}\{\delta_e\} = [P_e] - [P_e^s] \tag{36}$$

for surface elements, and

$$[K_e]\{\delta_e\} = [P_e] \tag{37}$$

for bulk elements, respectively, where $[K_e]$ is the stiffness matrix, and $[P_e]$ is the nodal force matrix of bulk elements.

The above finite element method is adopted here to investigate the deformation near a blunted crack tip with the effect of surface energy. In our calculations, the front tip of a semi-infinity crack is assumed to have the shape of a circular arc, and we take the following surface constants of aluminum [7]: $\lambda^s=6.842$ N/m, $\mu^s=-0.3755$ N/m, and $\tau^0=0$.

Our numerical simulations show that the stress distributions with surface elasticity effects have a good agreement with the predictions of linear elastic fracture mechanics except in a small vicinity of the crack tip, where the surface energy has a significant influence. Similar results were also obtained directly from atomic simulation [17]. The calculated circumferential stress σ_{yy}^p in Eq. (28) at the crack tip normalized by σ_{yy}^0 is plotted in Fig. 3 as a function of the root curvature radius ρ. It is seen that the analytical solution and the numerical result for the stresses at the crack tip

agree reasonably well. Therefore, the local analysis adopted in the present paper can capture the most prominent features of surface effects on the near-tip stresses and deformations.

6 Conclusions

In the present paper, we adopt an asymptotic method to investigate the effects of surface energy on the stresses near a crack tip with finite root radius. The analytical relations between the surface constants and the stresses at the crack tip are obtained. The results show that only when the curvature radius at the crack tip reduces to nanometers do the surface effects become significant. For mode-III cracks, surface energy does not affect the stresses at crack tips, while it does influence the stresses at a small distance ahead of the crack tip. For mode-I cracks, the surface energy evidently alters the stress magnitudes at the crack tips. The obtained analytical solution agrees reasonable well with the results of our finite element numerical simulations, in which the effects of surface energy have been incorporated. This study might be helpful for understanding some size-dependent fracture phenomena, especially for micro- or nanosized devices and systems.

Acknowledgment

The support from the National Natural Science Foundation of China (Grants No. 10602042, No. 10121202, and No. 10525210), the 973 project (Grant No. 2004CB619303), and the Program for NCET by the Ministry of Education of China are acknowledged.

References

[1] Buehler, M. J., and Gao, H. J., 2006, "Dynamical Fracture Instabilities Due to Local Hyperelasticity at Crack Tips," Nature (London), **439**, pp. 307–310.
[2] Buehler, M. J., Abraham, F. F., and Gao, H. J., 2003, "Hyperelasticity Governs Dynamic Fracture at a Critical Length Scale," Nature (London), **426**, pp. 141–146.
[3] Buehler, M. J., Gao, H. J., and Huang, Y. G., 2004, "Continuum and Atomistic Studies of the Near-Crack Field of a Rapidly Propagating Crack in a Harmonic Lattice," Theor. Appl. Fract. Mech., **41**, pp. 21–42.
[4] Abraham, F. F., Broughton, J. Q., Bernstein, N., and Kaxiras, E., 1998, "Spanning the Continuum to Quantum Length Scales in a Dynamic Simulation of Brittle Fracture," Europhys. Lett., **44**, pp. 783–787.
[5] Miller, R. E., and Shenoy, V. B., 2000, "Size-Dependent Elastic Properties of Nanosized Structural Elements," Nanotechnology, **11**, pp. 139–147.
[6] Shenoy, V. B., 2002, "Size-Dependent Rigidities of Nanosized Torsional Elements," Int. J. Solids Struct., **39**, pp. 4039–4052.
[7] Sharma, P., Ganti, S., and Bhate, N., 2003, "Effect of Surfaces on the Size-Dependent Elastic State of Nanoinhomogeneities," Appl. Phys. Lett., **82**, pp. 535–537.
[8] Cammarata, R. C., Sieradzki, K., and Spaepen, F., 2000, "Simple Model for Interface Stresses With Application to Misfit Dislocation Generation in Epitaxial Thin Films," J. Appl. Phys., **87**, pp. 1227–1234.
[9] Dingreville, R., Qu, J. M., and Cherkaoui, M., 2005, "Surface Free Energy and Its Effect on the Elastic Behavior of Nano-Sized Particles, Wires and Films," J. Mech. Phys. Solids, **53**, pp. 1827–1854.
[10] Gurtin, M. E., and Murdoch, A. I., 1975, "A Continuum Theory of Elastic Material Surfaces," Arch. Ration. Mech. Anal., **57**, pp. 291–323.
[11] Gurtin, M. E., Weissmuller, J., and Larche, F., 1998, "A General Theory of Curved Deformable Interfaces in Solids at Equilibrium," Philos. Mag. A, **78**, pp. 1093–1109.
[12] Yang, F. Q., 2004, "Size-Dependent Effective Modulus of Elastic Composite Materials: Spherical Nanocavities at Dilute Concentrations," J. Appl. Phys., **95**, pp. 3516–3520.
[13] Gao, W., Yu, S. W., and Huang, G. Y., 2006, "Finite Element Characterization of the Size-Dependent Mechanical Behaviour in Nanosystems," Nanotechnology, **17**, pp. 1118–1122.
[14] Sharma, P., and Ganti, S., 2004, "Size-Dependent Eshelby's Tensor for Embedded Nano-Inclusions Incorporating Surface/Interface Energies," ASME, ASME J. Appl. Mech., **71**, pp. 663–670.
[15] Duan, H. L., Wang, J., Huang, Z. P., and Karihaloo, B. L., 2005, "Size-Dependent Effective Elastic Constants of Solids Containing Nano-Inhomogeneities With Interface Stress," J. Mech. Phys. Solids, **53**, pp. 1574–1596.
[16] Wu, C. H., 1999, "The Effect of Surface Stress on the Configurational Equilibrium of Voids and Cracks," J. Mech. Phys. Solids, **47**, pp. 2469–2492.
[17] Horgland, R. G., Daw, M. S., and Hirth, J. P., 1991, "Some Aspects of Forces and Fields in Atomic Models of Crack Tips," J. Mater. Res., **6**, pp. 2565–2571.
[18] Creager, M., and Paris, P. C., 1967, "Elastic Field Equations for Blunt Cracks With Reference to Stress Corrosion Cracking," Int. J. Fract. Mech., **3**, pp. 247–252.
[19] Smith, E., 2004, "A Comparison of Mode I and Mode III Results for the Elastic Stress Distribution in the Immediate Vicinity of a Blunt Notch," Int. J. Eng. Sci., **42**, pp. 473–481.
[20] England, A. E., 1971, *Complex Variable Methods in Elasticity*, Wiley, New York.